ELSEVIER

Fluid Dynamics Research 20 (1997) 1–10

FLUID DYNAMICS RESEARCH

Large-eddy simulation of turbulence in the free atmosphere and behind aircraft

U. Schumann*,[1], A. Dörnbrack, T. Dürbeck, T. Gerz

DLR, Institut für Physik der Atmosphäre, Oberpfaffenhofen, D-82230 Wessling, Germany

Abstract

The method of large-eddy simulation has been used for a wide variety of atmospheric flow problems. This paper gives an overview on recent applications of this method to turbulence in the free atmosphere under stably stratified conditions. In particular, flows in the wake of aircraft are studied in light of the potential impact of aircraft exhausts on the chemical and climatological state of the atmosphere. It is shown that different profiles of heat and moisture in the initial conditions of a jet representing engine exhaust gases may cause larger water saturation and hence earlier contrail formation than assumed up to now. The instability of trailing vortices in the wake of an aircraft is simulated up to the fully turbulent regime. The vertical diffusivity of aircraft exhaust is large in the vortex regime and much smaller than horizontal diffusivities in the later diffusion regime. The three-dimensional formation of a critical layer and breaking of gravity waves is simulated.

Keywords: Large-eddy simulation (LES); Turbulence; Aircraft emissions; Contrail formation; Trailing vortices; Effective diffusivities; Breaking gravity waves

1. Introduction

The method of large-eddy simulation (LES) has been developed originally for applications in atmospheric sciences. In 1970, Deardorff (1970) presented the first successful LES for simulations of Poiseuille flows but soon applied the method to atmospheric boundary-layer flows, with shear and buoyancy effects (Deardorff, 1972). In the meantime, the method of LES has become standard for many kinds of applications, including flow simulations in the neutral atmospheric boundary layer (Andrén et al., 1994), the convective boundary layer (Nieuwstadt et al., 1993), and the stable boundary layer (Mason, 1994; Andrén, 1995). There are also many applications of LES to cloud motions, e.g. (Klemp and Wilhelmson, 1978). However, there are still relatively few applications with respect to flows in the free atmosphere (Fritts et al., 1994).

* Corresponding author.
[1] E-mail: ulrich.schumann@dlr.de.

0169-5983/97/$17.00
PII S0169-5983(96)00044-5

We distinguish between the troposphere (up to the tropopause, typically near 10 km altitude at mid-latitudes) and the stratosphere above. Above the boundary layer, the troposphere is usually stably stratified, except in cloud systems. A typical Brunt–Väisälä frequency of vertical oscillations in the stratified fluid is $N = 0.01\,s^{-1}$. The Richardson number $Ri = N^2/S^2$ is mostly above 0.25 (S = vertical velocity shear), i.e. above the limit of linear instability of stratified shear flows (Miles, 1961; Schumann and Gerz, 1995). In the stratosphere, N is typically $0.02\,s^{-1}$, and the Richardson number usually much larger than one. As a consequence, the atmosphere contains large regions which are essentially free of turbulence (in the sense of Kolmogorov with energy cascade from large to small scales) (Schumann et al., 1995). The free atmosphere region is more difficult to treat than boundary layer flows because of the wide and often undefined scale regime. The horizontal motion scales may cover the whole range from the Kolmogorov scale to the global scale. The vertical scales are usually much smaller than the height above the surface.

Many variants of LES have been developed, as reviewed in (Ciofalo, 1994), ranging from the classical Smagorinsky scheme, to high-order turbulence models (Schmidt and Schumann, 1989). In recent years, several problems in the Smagorinsky model have been identified and partly overcome, such as the adaptation of the Smagorinsky coefficient to transient flows or flows with strong local shear but little subgrid scale (SGS) mixing, which can be treated by dynamic SGS models (Germano et al., 1991; Ghosal et al., 1995). The impact of buoyancy forces can be accounted for using separate transport equations for the SGS kinetic energy (Schmidt and Schumann, 1989; Kaltenbach et al., 1994). Other problems result from the fact that the SGS stresses are related to the local deformation tensor only in a statistical sense. Random components contribute to backscatter of energy from SGS to larger scales. Related models have been proposed to account for backscatter (Mason, 1994; Mason and Thomson, 1992; Schumann, 1995).

However, in many applications, in particular remote from walls, the SGS fluxes are sufficiently small compared to the resolved fluxes so that the details of the SGS model hardly matter. In this case, we still prefer to use the simplest model as proposed by Smagorinsky to reduce the complexity of the model. Moreover, the simplest approach is often the most robust one and easiest to analyse. Usually, the theoretical base of SGS model requires that the grid scales are within the inertial subrange of turbulence. If a coarse LES does not resolve the essential energy and flux carrying flow elements, then an improvement in the SGS model rarely solves this problem. Instead, model limitations usually have to be overcome by increasing the numerical resolution or by principally changing the approach.

In recent years, considerable research efforts started to investigate the potential impact of aircraft emissions on the state of the atmosphere and possible consequences with respect to climate (Schumann, 1994). Supersonic aircraft were considered early (CIAP, 1975), but now subsonic aircraft are included also (Schumann, 1994; WMO, 1995). Emissions from aircraft engines include carbon dioxide, water vapour, nitrogen oxides, sulphur oxides, soot, and various other gases and particles. Aircraft fly mostly near the tropopause or in the lower stratosphere which is a region of particular sensitivity because of low temperature, low background concentrations, slow mixing rates, and large ozone concentration. Here, emissions may change the atmospheric ozone concentration, increase cloudiness, and enhance the greenhouse effect. Present subsonic traffic consumes about 6% of all petrol products and fuel consumption is expected to increase by 2–4% per year. Hence, emissions from aircraft increase with possibly enhanced effects. For sustained development of economy and for ecology, it is of utmost importance to provide reliable assessments. Up to now, much work is in progress, but the answers given are yet very preliminary (WMO, 1995).

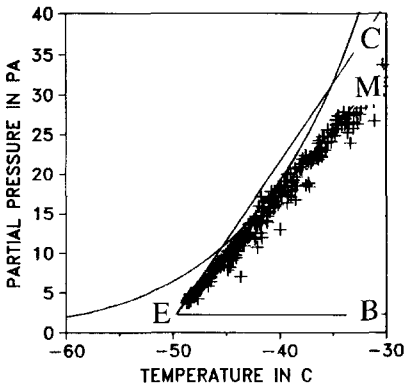

Fig. 1. Liquid saturation pressure (curve) and mixing lines from core engine (C), bypass (B) and a fully mixed exit condition (M) to the state in the environment (E). The crosses indicate the values in individual grid cells after 0.09 s.

In this paper, we will present examples of LES results which were developed within projects concerned with the impact of air traffic, although none of these specific studies are meant to give a comprehensive answer to the overall question.

2. Contrail formation in the jet of a turbofan engine

As an example of application of LES to atmospheric flow problems, we consider the formation of contrails. In order to assess the impact of contrails one needs to know the conditions under which contrails form. According to the classical thermodynamic Schmidt/Appleman criterion (Appleman, 1953; Schumann, 1996), contrails form in the engine exhaust jet when mixing between the hot and humid exhaust gases and cold and dry ambient air leads to a mixture reaching saturation with respect to water so that cloud droplets form on suitable cloud condensation nuclei. Short-lived contrails form in dry air while persistent contrails may get formed in frost saturated air with relative humidity above ice saturation and below liquid saturation. In a diagram as in Fig. 1, depicting the water partial pressure as a function of temperature, isobaric mixing between ideal gases follows along a straight line from the engine exit conditions to the environmental state. Contrails may form when the mixing line M–E touches the saturation pressure curve shown in Fig. 1. This requires that the temperature in the environment is below a certain threshold value which is about −50°C in this case.

This analysis assumes that heat and water are added to the plume and mix similarly, i.e. with equal diffusivities and similar initial conditions. The diffusivities for heat and water vapour are the same at high Reynolds numbers. However, modern turbofan engines emit water vapour only with the core engine exhaust while part of the thermal energy is transferred to the bypass air by means of the work performed by the fan turbine. If gases from the moist core exhaust would mix directly with ambient air before getting diluted with bypass air then mixing follows the steeper line C–E indicated in Fig. 1, and hence much higher water saturation may be reached. This offers the possibility that contrails form at temperatures higher than predicted by the classical theories.

Of course, core exhaust can mix with ambient air directly only when turbulent eddies from the core jet penetrate the bypass annular jet without essential mixing. It is not clear whether such

penetrations are possible. The passive scalar dispersion and mixing has been studied experimentally for two scalars which were introduced with different initial profiles into a turbulent jet (Tong and Warhaft, 1995). The scalar fields become similar after a few eddy turnover times of the jet. These experiments were performed for a single jet without a coannular jet. We do not know of studies of mixing between two scalar fields in coannular jets typical for aircraft conditions. One-dimensional turbulence models (Kärcher, 1994) assume continuous mixing between core exhaust gases, bypass air and ambient air, without penetrative mixing. Therefore, we performed a LES study of coannular turbulent jets with two passive scalars to investigate whether such penetrative mixing occurs.

The jets are represented by a parallel flow in a rectangular computational domain with periodic boundary conditions in all three directions. The simulation describes the mixing of the jet air with ambient air as a function of time in this domain. Hence, the spatial spreading of the expanding jet is approximated by a temporal spreading. This kind of approximation should be suitable for a study of the basic mixing process.

The initial conditions of the jet model equal the conditions for an experiment with a specific aircraft (the ATTAS aircraft of DLR, a twin-engine jet-aircraft of moderate size) (Busen and Schumann, 1995): ambient pressure 302.3 hPa, temperature −49.7°C, relative humidity 34%, aircraft speed 115 m s^{-1}, fuel flow rate 125 g s^{-1} and thrust 6.4 kN per engine, burning kerosene with specific combustion heat 43 MJ kg^{-1}, emitting 1.206 mass units of water vapour per mass unit of fuel. This case is of interest because a contrail was observed to form about 30 m (jet age 0.26 s) behind the aircraft. In order to form liquid particles large enough for a visible contrail in the short time as observed, the relative humidity must be well above 100%. But the classical thermodynamic analysis for the given conditions shows that the maximum relative humidity with respect to liquid saturation reaches only 95% (with 7% uncertainty from the ambient temperature and humidity data), which left the observed contrail formation basically unexplained. The curve C–E would allow for a maximum relative humidity of 113%.

The computational domain is of size 12.8×6.4^2 m^3, the grid includes 128×64^2 grid cells, with equal grid spacing (0.1 m) in all three directions. The initial core jet extends over 4×4 grid cells, and the bypass jet is within the 8×8 grid cells surrounding the core jet along the X-axis, with cross-sections of 0.16 and 0.48 m^2. Because of the rather coarse resolution, the jets are initialised with square cross-sections but become circular soon during the simulations. Relative to ambient air, the initial values specify differences in velocity of 312 and 142 m s^{-1}, temperature of 427 and 35.4 K, and water vapour concentration of 17.4 g kg^{-1} and 0, in the jet and the bypass, respectively.

The simulation treats the velocity field in the Boussinesq approximation (constant density of 0.471 kg m^{-3}) and assumes constant specific heat capacity of 1004 J kg^{-1} K^{-1}. The initial flow is perturbed with random motions in the bypass and core jet while the ambient air is assumed to be without turbulence initially. We expect that the probability of penetration of core air through the bypass coannular jet air increases with the ratio of jet and bypass velocity and the magnitude of initial velocity fluctuations. The disturbances are kept small so that the results may underestimate possible core air penetrations. The initial velocity disturbance is composed of Gaussian random numbers of amplitude 3×10^{-4} times the core jet velocity and wavy variations along the jet axis in the 3 first axial wave numbers with an amplitude of about 3% of the jet velocity. Temperature and water vapour concentration values are without initial disturbances in these simulations. The numerical method is the same as described in (Gerz et al., 1989; Gerz and Palma, 1994). It uses a second-order finite difference scheme together with the Smagorinsky model ($c_s = 0.1$, turbulent Prandtl number of

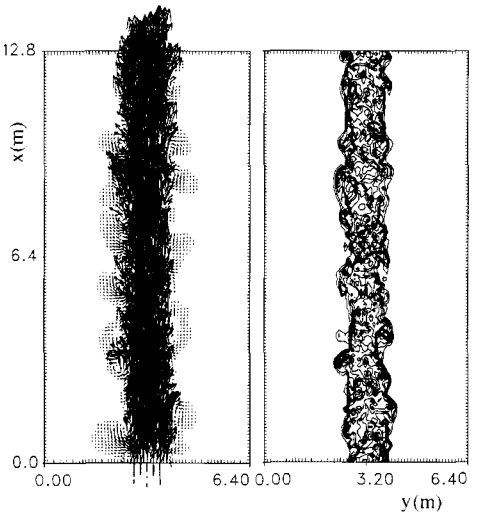

Fig. 2. Jet velocity field (left) and temperature field (right) in a plane of the jet axis at time 0.09 s. The initial dimensions of the core and bypass jet are indicated at the bottom axis.

0.419). The equations are integrated with the Adams–Bashforth scheme (maximum Courant number 0.31).

The turbulent jet expands quickly by mixing. After 0.09 s (900 time steps), the flow structure, see Fig. 2, exhibits turbulent eddies which penetrate into the calm ambient air. Some eddies get ejected from the turbulent region quite far into the ambient air. This makes it reasonable that core air may get transported through the bypass air with only partly mixing. Within the time of 0.3 s, the jet expands to a diameter of about 2.5 m, which is realistic when compared to the observations (Busen and Schumann, 1995).

The water vapour concentration field looks similar to the temperature field (not plotted, therefore). From the results we compute the local water vapour partial pressure and the relative humidity. The humidity values are maximum at the outside of the turbulent jet. The absolute maximum is found at time 0.09 s. For this time, and for a selection of three cross-sections through the plane, Fig. 1 depicts the local water vapour partial pressure values as computed in the jet. We see that the partial pressure at some grid points exceeds the saturation curve. The relative humidity reaches maximum values of 1.07, i.e. 12% higher values than for homogeneous emissions, only little less than the maximum value possible (1.13), clearly exceeding liquid water saturation. The quantitative result may be uncertain because of numerical dispersion with the scheme that does not preserve monotonicity. This should be checked by using slightly smoothed initial conditions in the future. Moreover, the numerical scheme causes some numerical diffusion. However, any diffusion process will reduce the differences between bypass and core exhaust gases. Hence, the simulation might underestimate the possible increase in relative humidity due to inhomogeneous mixing.

The result shows that a fraction of the core air gets mixed directly with ambient air and produces saturation values higher than for the case when core and bypass air are initially mixed completely. Hence, contrails may form even under conditions where no contrails would be expected from the classical Schmidt/Appleman criterion.

3. Instability of trailing vortices

The lift-generating circulation around the wing and the finite length of wings cause that a pair of trailing vortices leave the wing tips and roll up to steady parallel vortices within a few span widths after an aircraft (CIAP, 1975; Scorer and Davenport, 1970). Much (but not all) of the aircraft emissions get captured into the centre of these trailing vortices. Hence, the length of the visible contrail and the chemistry between various emission products and ambient air depends strongly on the stability of these vortices. The vortices become unstable after some time due to the linear Crow instability of the interacting vortices (Crow, 1970). Soon thereafter, contrails break down into turbulent motions. Little is known about the details of this secondary instability.

Therefore, we performed a LES of the vortex wake and the exhaust distribution left by a cruising aircraft (B747) in a stably stratified atmosphere (Gerz and Ehret, 1996). The simulations cover the period from the jet regime (age of 3 s) until the early dispersion regime (120 s). (The regimes were defined in (CIAP, 1975.)) The method used is the LES code as described in (Kaltenbach et al., 1994; Gerz and Palma, 1994) with the Smagorinsky SGS model. The model domain covers 184 m along the vortex lines and 154 m in the two cross-directions, using 192×160^2 grid cells. The vortex core radius is 3.4 m. The grid spacing is 0.96 m in all three coordinates. The code is initialised with the flow state of the wingtip vortices and the distribution of the exhaust provided by a 3d vortex filament method for a B747 (Ehret and Oertel, 1994). The turbulent air generated in the boundary layer at the aircraft wing is trapped in the trailing vortices. This initial turbulence is simulated with a three-dimensional random perturbation field added to the vortex flow field. The perturbation reaches its maximum value of 14% of the swirl velocity at the core radius and decays exponentially for smaller and larger radii. The atmosphere is represented by a motionless and stably stratified fluid with $N = 0.02\,\mathrm{s}^{-1}$.

The simulations show that the vortex pair travels downwards leaving a turbulent wake above due to detrainment of air in the vortex cores. The turbulent detrainment is enforced by buoyancy of the initially warm exhaust air and by buoyancy induced by vertical motions of vortex air relative to the stratified ambient air. The exhaust concentration maxima are found around the vortex cores. At about $\frac{1}{4}$ of the buoyancy period (75 s), the vortices reach a maximum depth of 126 m below flight level and the swirl around the cores ceases. Hence, the simulations extend from the vortex regime into the dispersion regime (CIAP, 1975). At this stage we observe a weak upwelling motion of detrained air, whereas the vortices themselves do not move upward since their reservoir of rotational energy creates a downward motion by mutual induction which compensates buoyancy forces. As a consequence, the rotational energy decays resulting in a quick vortex dissolution.

Fig. 3 illustrates the evolution of the Crow instability. Two initially parallel vortex cores, here indicated by the vorticity component pointing in flight direction, start to bend sinusoidally in a vertically skewed plane until they contact in the lower turning point which results in a quick destruction of the vortex. Although the details of this instability depend on the axial domain size, we see that LES can be used to investigate this instability.

An analysis of the dispersion of a passive tracer with these motions shows that the tracers get diffused mainly vertically with an effective diffusivity which varies in time between 4 and $40\,\mathrm{m}^2\,\mathrm{s}^{-1}$ with very little horizontal diffusion. This behaviour is confirmed by photos and Lidar observations (Freudenthaler et al., 1994). After vortex collapse, the plume grows mostly horizontally as will be shown below.

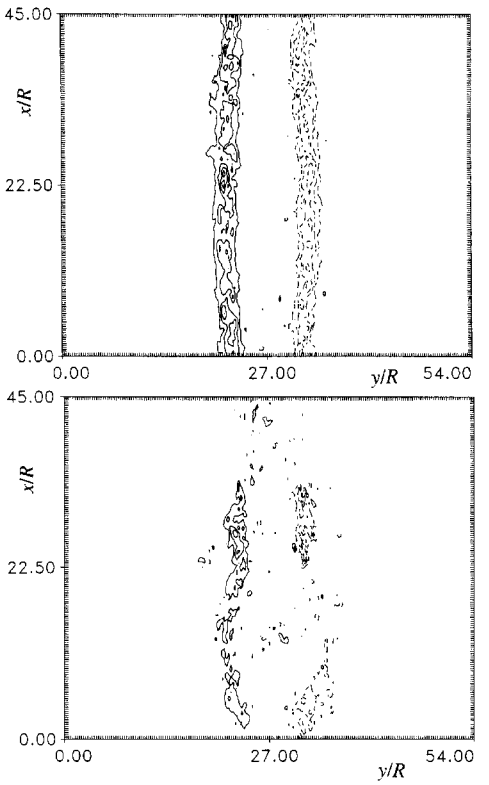

Fig. 3. Horizontal cross-sections showing the instantaneous field of wake vorticity ω_x in jet direction after 72 s (top) and 112 s (bottom). The coordinates are normalised with the vortex core radius $R = 3.4$ m.

4. Effective diffusivities after decay of the aircraft induced flows

After a time of several minutes, the vertical motions and the turbulence induced by the aircraft cease. Thereafter, the dispersion of emissions is controlled by atmospheric motions.

Recently, we have determined the horizontal and vertical diffusivities for dispersion of exhaust plumes from airliners at cruising altitudes from nitric oxide concentrations and turbulence data measured in situ using a research aircraft (Schumann et al., 1995). The measurements took place 5 to 100 min after emission of the exhaust from airliners at about 9.4 to 11.3 km altitude, near the tropopause, in the North-Atlantic flight corridor. The ambient atmosphere was stably stratified with bulk Richardson numbers greater than 10. The range of the plume data suggests vertical diffusivity values between 0 and $0.6\,m^2\,s^{-1}$. The turbulence data show that the air motions were strongly anisotropic with weak vertical velocity fluctuations. The turbulence spectra show no Kolmogorov inertial range and very small dissipation rates. This implies very small vertical diffusivities (Schumann and Gerz, 1995). The horizontal diffusivities of the plumes varied between 5 and $20\,m^2\,s^{-1}$ (Schumann et al., 1995).

In order to identify the impact of stratification and shear on the effective diffusivities, LES have been performed, first without shear (Dürbeck and Gerz, 1995). The SGS model uses a transport

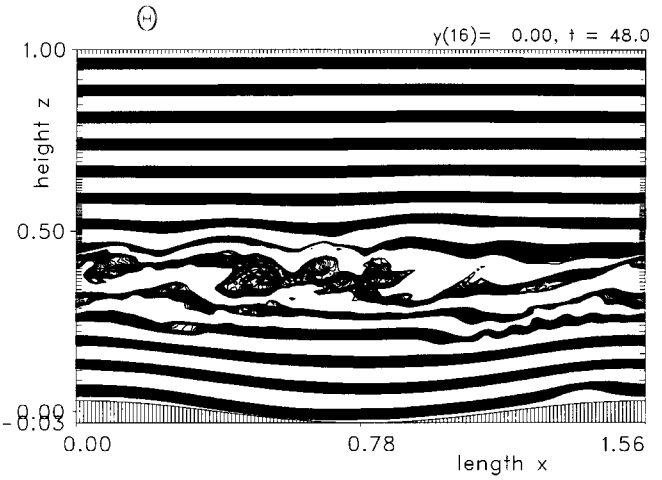

Fig. 4. Horizontal cross-section showing the instantaneous field of potential temperature for a breaking gravity-wave event. The coordinates are normalised with the domain height.

equation for the SGS kinetic energy to account for decaying and stratified turbulence (Gerz and Palma, 1994). The LES treats a domain of $4.3 \times 1.1^2\,\mathrm{km}^3$ with up to 320×80^2 grid points. The exhaust plumes of aircraft are represented by line sources with Gaussian cross-sections. The Brunt–Väisälä frequency is varied between 0.006 and $0.03\,\mathrm{s}^{-1}$. The results show that the effective horizontal diffusion coefficient lies between 11 and $21\,\mathrm{m}^2\,\mathrm{s}^{-1}$, depending on the level of stratification. The vertical diffusivities range from 2.3 to $0.37\,\mathrm{m}^2\,\mathrm{s}^{-1}$ in the beginning of the diffusion process, and amount to values which are near $0.15\,\mathrm{m}^2\,\mathrm{s}^{-1}$ for all stratifications later. It appears that the LES results are in close agreement with the experimental observations. LES studies of cases with shear are under progress.

5. Breaking gravity waves

The measurements and simulations as described above show weak or decaying turbulence under stably stratified situations at large Richardson numbers. However, it is known that sometimes very strong local turbulent events may arise even under stably stratified conditions.

Such events may arise from breaking gravity waves (Fritts et al., 1994) for various reasons. Breaking often results from upward travelling gravity waves with certain horizontal phase speed that interact with the mean flow at critical levels where the mean flow speed equals the phase speed of the waves.

In order to understand details of the breaking of gravity waves and the resulting turbulence, we studied the interaction of an internal gravity wave with a critical layer and the subsequent generation of turbulence by overturning waves using LES (Dörnbrack et al., 1995), see Fig. 4. The simulation describes the flow of a stably stratified Boussinesq fluid above a wavy bottom surface and below a flat top surface, both without friction and adiabatic. Between the surfaces a uniform shear flow is assumed with zero mean flow, i.e., there is flow from right to left near the bottom surface and from left to right near the top surface. The LES method is described in (Dörnbrack et al., 1995; Krettenauer

and Schumann, 1992). It is applied for a Reynolds number of 50 000, with $150 \times 30 \times 96$ grid cells. The flow over the wavy surface induces gravity waves which travel upwards up to the level of zero flow velocity. This is the critical level because the phase speed of the gravity waves is also zero. The simulations show how the critical layer develops in detail, how an overturning gravity wave forms which finally breaks down into turbulence. The transition occurs with coherent secondary rolls with axis in the downstream direction. Details of the turbulence intensity have been determined (Dörnbrack et al., 1995). Such data provide general background data to finally parameterise turbulence due to breaking gravity waves, although we are still far away from establishing generally applicable models for this purpose.

6. Conclusions

The method of LES has been developed for more than 25 years. Certainly, there are still many topics requiring further refinement of the method itself, in particular, for flows near wall surfaces and for complex geometries. However, the method is mature enough to be applied to a wide variety of problems, in particular, to cases where the flow structure per se is of interest. We have presented examples of LES applications to atmospheric flow problems related to ongoing projects dealing with the impact of aircraft emissions on the atmosphere. Such questions cannot be answered by LES alone but require the combination with other model studies and experimental investigations. Flows in the wake of aircraft, including the jet, vortex, dispersion, and diffusion regimes, and contrail processes, seem to be within the scope of present LES methods and will obtain increasing interest in the coming years.

References

Andrén, A., A. Brown, J. Graf, P.J. Mason, C.-H. Moeng, F.T.M. Nieuwstadt and U. Schumann (1994) Large-eddy simulation of a neutrally stratified boundary layer: a comparison of four computer codes, Q. J. Roy. Meteorol. Soc. 120, 1457–1484.

Andrén, A. (1990) The structure of stably stratified atmospheric boundary layers: a large-eddy simulation study, Q. J. Roy. Meteorol. Soc. 121, 961–985.

Appleman, H. (1953) The formation of exhaust condensation trails by jet aircraft, Bull. Amer. Meteorol. Soc. 34, 14–20.

Busen, R. and U. Schumann (1995) Visible contrail formation from fuels with different sulfur contents, Geophys. Res. Lett. 22, 1357–1360.

CIAP (1975) The stratosphere perturbed by propulsion effluents, CIAP Monogr. 3, Departm. Transport., Washington, DC, DOT-TST-75-53.

Ciofalo, M. (1994) Large-eddy simulation: a critical survey of models and applications, Advances in Heat Transfer, Vol. 25 (Academic Press, New York) 321–419.

Crow, S.C. (1970) Stability theory for a pair of trailing vortices, AIAA J. 8, 2172–2179.

Deardorff, J.W. (1970) A numerical study of three-dimensional turbulent channel flow at large Reynolds numbers, J. Fluid Mech. 41, 453–480.

Deardorff, J.W. (1972) Numerical investigation of neutral and unstable planetary boundary layers, J. Atmos. Sci. 29, 91–115.

Dörnbrack, A., T. Gerz and U. Schumann (1995) Turbulent breaking of overturning gravity waves below a critical level, Appl. Sci. Res. 54, 163–176.

Dürbeck, T. and T. Gerz (1995) Large-eddy simulation of aircraft exhaust plumes in the free atmosphere: effective diffusivities and cross-sections, Geophys. Res. Lett. 22, 3203–3206.

Ehret, T. and H. Oertel (1994) Numerical simulation of the dynamics and decay of trailing vortices including pollutants from air traffic, in: Proc. Intern. Sci. Coll. Impacts of Emissions from Aircraft and Spacecraft upon the Atmosphere, DLR-Mitt. 94-06, 268–273.

Freudenthaler, V., F. Homberg and H. Jäger (1994) Ground based mobile scanning Lidar for remote sensing of contrails, in: Proc. Intern. Sci. Coll. Impacts of Emissions from Aircraft and Spacecraft upon the Atmosphere, DLR-Mitt. 94-06, 407–411.

Fritts, D.C. et al. (1994) Gravity breaking in two and three dimensions. 2: three-dimensional evolution and instability structure, J. Geophys. Res. 99, 8109–8123.

Germano, M., U. Piomelli, P. Moin and W.H. Cabot (1991) A dynamic subgrid-scale eddy viscosity model, Phys. Fluids A 3, 1760–1765.

Gerz, T., U. Schumann and S.E. Elghobashi (1989) Direct numerical simulation of stratified homogeneous turbulent shear flows, J. Fluid Mech. 200, 563–594.

Gerz, T. and J.M.L.M. Palma (1994) Sheared and stably stratified homogeneous turbulence: comparison of DNS and LES, in: Direct and Large-Eddy Simulation, ed. P. Voke et al. (Kluwer, Dordrecht) 145–156.

Gerz, T. and T. Ehret (1996) Wake dynamics and exhaust distribution behind cruising aircraft, in: The Characterisation and Modification of Wakes from Lifting Vehicles in Fluids, Proc. CP-584, 78th Fluid Dynamics Panel Symp., Trondheim, Norway, 20–23, 35.1–35.12.

Ghosal, S., T.S. Lund, P. Moin and K. Akselvoll (1995) A dynamic localization model for large-eddy simulation of turbulent flows, J. Fluid Mech. 286, 229–255.

Kärcher, B. (1994) Transport of exhaust products in the near trail of a jet engine under atmospheric conditions, J. Geophys. Res. 99, 14509–14517.

Kaltenbach, H.-J., T. Gerz and U. Schumann (1994) Large-eddy simulation of homogeneous turbulence and diffusion in stably stratified shear flow, J. Fluid Mech. 280, 1–40.

Klemp, J.B. and R.B. Wilhelmson (1978) The simulation of three-dimensional convective storm dynamics, J. Atmos. Sci. 35, 1070–1096.

Krettenauer, K. and U. Schumann (1992) Numerical simulation of turbulent convection over wavy terrain, J. Fluid Mech. 237, 261–299.

Mason, P.J. and D.J. Thomson (1992) Stochastic backscatter in large-eddy simulations of boundary layers, J. Fluid Mech. 242, 51–78.

Mason, P.J. (1994) Large-eddy simulation: a critical review, Q. J. Roy. Meteorol. Soc. 120, 1–26.

Miles, J.W. (1961) On the stability of heterogeneous shear flows, J. Fluid Mech. 10, 496–508.

Nieuwstadt, F.T.M., P.J. Mason, C.-H. Moeng and U. Schumann (1993) Large-eddy simulation of the convective boundary layer: a comparison of four computer codes, in: Turbulent Shear Flows 8, eds. F. Durst et al. (Springer, Berlin) 343–367.

Schmidt, H. and U. Schumann (1989) Coherent structure of the convective boundary layer derived from large-eddy simulations, J. Fluid Mech. 200, 511–562.

Schumann, U. (1994) On the effect of emissions from aircraft engines on the state of the atmosphere. Ann. Geophys. 12, 365–384.

Schumann, U. (1995) Stochastic backscatter of turbulence energy and scalar variance by random subgrid-scale fluxes, Proc. Roy. Soc. London A 451, 283–318 and 811.

Schumann, U. and T. Gerz (1995) Turbulent mixing in stably stratified shear flows, J. Appl. Meteorol. 34, 33–48.

Schumann, U., P. Konopka, R. Baumann, R. Busen, T. Gerz, H. Schlager, P. Schulte and H. Volkert (1995) Estimate of diffusion parameters of aircraft exhaust plumes near the tropopause from nitric oxide and turbulence measurements, J. Geophys. Res. 100, 14147–14162.

Schumann, U. (1996) On conditions for contrail formation from aircraft exhausts, Meteorol. Z., N. F. 5, 4–23.

Scorer, R.S. and L.J. Davenport (1970) Contrails and aircraft downwash, J. Fluid Mech. 43, 451–464.

Tong, C. and Z. Warhaft (1995) Passive scalar dispersion and mixing in a turbulent jet, J. Fluid Mech. 292, 1–38.

WMO (1995) Scientific assessment of ozone depletion: 1994, Global Ozone Research and Monitoring Project, Report No. 37, World Meteorological Organization, C. P. No. 5, CH-1211 Geneva 20, Switzerland.